Check for updates

Special Collection: Carbon Emissions and Sustainable Development in Developing Countries

ENERGY EXPLORATION & EXPLOITATION

Energy Exploration & Exploitation
2021, Vol. 39(5) 1532–1550
© The Author(s) 2020
DOI: 10.1177/0144598720927078
journals.sagepub.com/home/eea
SAGE

Techno-economic analysis of intermediate hydrocarbon injection on coupled CO_2 storage and enhanced oil recovery

Jinhyung Cho[1], Moon S Jeong[2], Young W Lee[2], Hye S Lee[2] and Kun S Lee[2]

Abstract

This study proposes economic evaluation of CO_2 geological storage with enhanced oil recovery. The procedures consider capital expenditures and operating costs of infrastructures and revenues from oil recovery and carbon tax credits. Extensive CO_2 geological storage with enhanced oil recovery simulations was conducted to determine the most promising scenario among cases, where miscibility was controlled by the addition of liquefied petroleum gas. The addition of liquefied petroleum gas into a CO_2 injection stream can accelerate reduction of oil viscosity, interfacial tension, and oil density, which cause improved displacement efficiency. The larger was the amount of liquefied petroleum gas injected, the greater was the miscibility due to minimum miscibility pressure reduction, resulting in higher oil recovery and less CO_2 sequestration. Although liquefied petroleum gas addition enhances the performance of CO_2 enhanced oil recovery, economic analysis should be conducted for CO_2 geological storage with enhanced oil recovery due to the higher price of liquefied petroleum gas than that of CO_2. Net present value decreased from liquefied petroleum gas mole fraction of 0–2% and started to increase from mole fraction 2–13% due to the miscibility effect. Then, net present value started to decrease, because the purchasing and injecting prices of the required liquefied petroleum gas exceeded that of the oil produced. Economic evaluation showed that addition of 13% liquefied petroleum

[1]Severe Storm Research Center, Ewha Womans University, Seodaemun-gu, Seoul, Republic of Korea
[2]Department of Earth Resources and Environmental Engineering, Hanyang University, Seongdong-gu, Seoul, Republic of Korea

Corresponding author:
Kun S Lee, Department of Earth Resources and Environmental Engineering, Hanyang University, 222 Wangsimni-ro, Seongdong-gu, Seoul 04763, Republic of Korea.
Email: kunslee@hanyang.ac.kr

Creative Commons CC BY: This article is distributed under the terms of the Creative Commons Attribution 4.0 License (https://creativecommons.org/licenses/by/4.0/) which permits any use, reproduction and distribution of the work without further permission provided the original work is attributed as specified on the SAGE and Open Access pages (https://us.sagepub.com/en-us/nam/open-access-at-sage).

gas was the most promising scenario, with a net present value of 91 MM$. Thus, we confirmed an optimum liquefied petroleum gas concentration in the CO_2 geological storage with enhanced oil recovery process.

Keywords
CCUS, CO_2 EOR, LPG, economic feasibility, miscibility

Introduction

It is expected that world gross domestic product (GDP) will double from 2016 to 2040 because of the economic expansion and development of non-Organisation for Economic Co-operation and Development (OECD) and OECD countries; more dominant from developing countries (ExxonMobil, 2018). According to the report, the energy consumption will increase in every sector of transportation, industries, and electricity generation mainly due to the development in non-OECD. However, because of the environmental effect, the portion of coal use in global energy mix will decrease, and the demand of oil in transportation sector and gas and renewables in electricity generation sector will increase. Because of the complexity of the relationship from economic growth to energy, many researches have been conducted (Appiah, 2018; Tiba and Omri, 2017; Walheer, 2018). Showing how economies react to an unexpected reduction in oil production, Bastianin et al. (2017) emphasized the importance of energy security with oil.

Worldwide oil demand and carbon emissions are predicted to increase gradually until 2040, and good solutions for this issue are CO_2 enhanced oil recovery (EOR) and CO_2 geological storage (Alvarado and Manrique, 2010; BP, 2018). The main drawback of CO_2 storage in an aquifer is lack of commercial value; CO_2 EOR can resolve this problem by enhancement of oil production as part of the carbon capture, utilization, and storage processes (Leung et al., 2014). Coupled CO_2 storage and EOR (CCS–EOR) can propose commercial opportunities for oil producers and ensure the geological storage of large quantities of CO_2. Nearly, 80 $MtCO_2$ is already being used for CCS–EOR each year (IEA, 2019). CO_2-EOR is one of the most effective EOR methods and is performed by injecting CO_2, which acts as a solvent to reduce oil viscosity, interfacial tension (IFT), and oil density. This can extend the production period by 15–20 years, with oil recovered at 15–25% of the original oil in place (Dong et al., 2000; Yongmao et al., 2004).

There have been a number of attempts to combine CCS and EOR. Ettehadtavakkol et al. (2014) focused on the sensitivity of economic parameters with various water alternating gas (WAG) ratios during CCS–EOR. However, the effects of reservoir in-situ condition controls, such as miscibility adjustment, impurities in the CO_2 stream, and IFT change-triggered relative permeability curve alteration, on net present value (NPV) have not been considered. Hasan et al. (2015) designed a CO_2 utilization through CO_2 EOR considering economic parameters, not considering fluid flow mechanisms and the operating cost for miscibility while the process. Rognmo et al. (2019) provided an experimental approach to test and upscale a CO_2 foam injection as one of injection schemes for CCS–EOR without the economic analysis. Nunez-Lopez et al. (2019) performed reservoir simulation studies with various CO_2 injection scenarios for CCS–EOR. However, they only focus the oil production

and CO_2 storage without economic analysis and constant miscibility mechanisms. Those studies focused only on in-situ mechanisms and performances and neglected the economics of field operation including CO_2 capture, transportation, and injection.

Since the optimum operating design and condition to enhance the performance of CCS–EOR at each reservoir is different, it is necessary to develop site-specific design based on economic analysis for the field application. To overcome the limitations of previous studies, CCS–EOR was performed from the viewpoint of economics to derive the most promising scenario with variable miscibility conditions with liquefied petroleum gas (LPG) and economic parameters. Capital expenditures (CAPEX) and operating costs (OPEX) of operation and revenues from oil recovery and carbon tax credits were adopted to evaluate NPV, because it is one of the most practical tools used in investment analysis for evaluating profitability, also known as economic decision criteria (Abdel-Aal and Al Sahlawi, 2013).

First, a numerical study for CCS–EOR was conducted. Oil recovery and sequestered CO_2 by each mechanism of solubility trapping, residual trapping, and free CO_2 under different miscibility conditions were examined. The results of the fluid model matched the experimental data. Then, minimum miscibility pressure (MMP) was calculated from a slim-tube simulation. The amount of LPG added into the injection gas was controlled to change miscibility conditions. Addition of LPG into the CO_2 stream can lower the MMP, which accelerates the reduction of oil viscosity, IFT, and oil density. The effects of IFT change due to miscibility increase were included by modification of liquid–gas relative permeability curves, which led to different flow regimes and performances under different miscibility conditions. Finally, NPVs of various miscibility conditions, which were adjusted by pressure control and LPG addition, were analyzed.

Numerical model

Residual and solubility trappings

The relative permeability curve follows different paths with imbibition or drainage processes, which causes the hysteresis effect. For the WAG process, CO_2 can be stored as water imbibes into a reservoir. Numerous studies have established equations to explain this phenomenon (Blunt, 2000; Jerauld, 1997; Killough, 1976; Land, 1968; Larsen and Skauge, 1998; Lenhard and Oostrom, 1998; Lenhard and Parker, 1987). The Land model, which is the most widely used empirical trapping model and base for subsequent hysteresis models, was used in this study. The hysteresis effect on gas relative to permeability is calculated as follows (equations (1) to (3))

$$k_{rg}(S_g) = k_{rg}(S_g), \text{ during drainage} \tag{1}$$

$$k_{rg}(S_g) = k_{rg}(S_{g,\ \text{shifted}}), \text{ during imbibition, and} \tag{2}$$

$$S_{g,\text{shifted}} = S_{gr} + \frac{(S_g - S_{grh})(S_{gh} - S_{gr})}{S_{gh} - S_{grh}} \tag{3}$$

where

k_{rg} = relative permeability of gas, and

$S_{gh} = S_g$ at the shift to imbibition.

S_{grh} is the value of S_{gr} corresponding to S_{gh} via Land's equation (Land, 1968) as follows

$$\frac{1}{S_{gr\max} - S_{gr}} - \frac{1}{S_{g\max} - S_{gr}} = \frac{1}{S_{grh} - S_{gr}} - \frac{1}{S_{gh} - S_{gr}} \quad \text{and} \tag{4}$$

$$S_{g\max} = 1 - S_{wr} \tag{5}$$

where

S_{wr} = connate water saturation.

$S_{gr\max}$ is calculated using the Holtz equation as shown below (Holtz, 2002)

$$S_{gr\max} = -0.9696\phi + 0.5473 \tag{6}$$

where ϕ is porosity.

The Peng–Robinson EOS (1976) was applied to calculate the fugacities of components in the oil and gas phases and to determine CO_2 solubility and phase behavior of the fluid model with the reservoir oil and CO_2. To calculate the fugacity of CO_2 in the aqueous phase, Henry's law was used (Li and Nghiem, 1986)

$$f_{iw} = y_{iw} H_i \quad \text{and} \tag{7}$$

$$\ln H_i = \ln H_i^* + \frac{\bar{v}_i (p - p^*)}{RT} \tag{8}$$

where

H_i = Henry's constant of component i (kPa);

y_{iw} = mole fraction of component i in the aqueous phase;

p = pressure (kPa);

p^* = reference pressure (kPa);

H_i^* = Henry's constant for component i at pressure p^* and temperature T (kPa);

T = temperature, (K); and

$\bar{v}_i$ = partial molar volume of component i at infinite dilution as computed by Harvey's correlation (1996) (cm^3/mol).

Relative permeability alteration

Decrease of IFT between oil and gas improves relative permeability for gas and oil (Araujo et al., 2001; Bardon and Longeron, 1980; Jamaloei, 2015; McDougall et al., 1997). The relative curves for oil and gas are linear functions of oil and gas saturations in miscible conditions. The modified relative permeability curves for oil and gas are denoted as k_{rot} and k_{rgt}, respectively

$$k_{rot} = f k_{ro} + (1 - f) k_{rh} \frac{S_o}{1 - S_w} \tag{9}$$

$$k_{rgt} = fk_{rg} + (1-f)k_{rh}\frac{S_g}{1-S_w} \quad \text{and} \tag{10}$$

$$k_{rh} = 0.5\left[k_{row}(S_w) + k_{rg}(S_g)\right] \tag{11}$$

where

$$f = 1\begin{cases} 1, & \text{where } \sigma > \sigma_o \\ \left(\frac{\sigma}{\sigma_o}\right)^n, & \text{where } \sigma \le \sigma_o \end{cases}$$

where σ is the IFT between oil and gas in dynes per centimeter calculated using the MacLeod–Sugden correlation (Reid et al., 1977), while σ_o is the reference IFT for relative permeability calculations and n is the exponent for gas-oil relative permeabilities, which was set as 0.1.

Economic parameters calculation

For CCS–EOR, it is important to examine not only reservoir performances, but also infrastructure-related costs that critically affect economic feasibility. Figure 1 shows a brief schematic of CCS–EOR. Here, CO_2 is captured from facilities, such as a pulverized coal and integrated gasification combined cycle (IGCC) plant, boosted for transport to the reservoir site through a pipeline, and injected with the help of surface facilities, such as a pump. Every step needs economic evaluation for successful development in the oil field.

There are several other costs that affect the cost calculation, such as surface equipment lease fee and minor costs for screening, contracts, insurance, and monitoring.

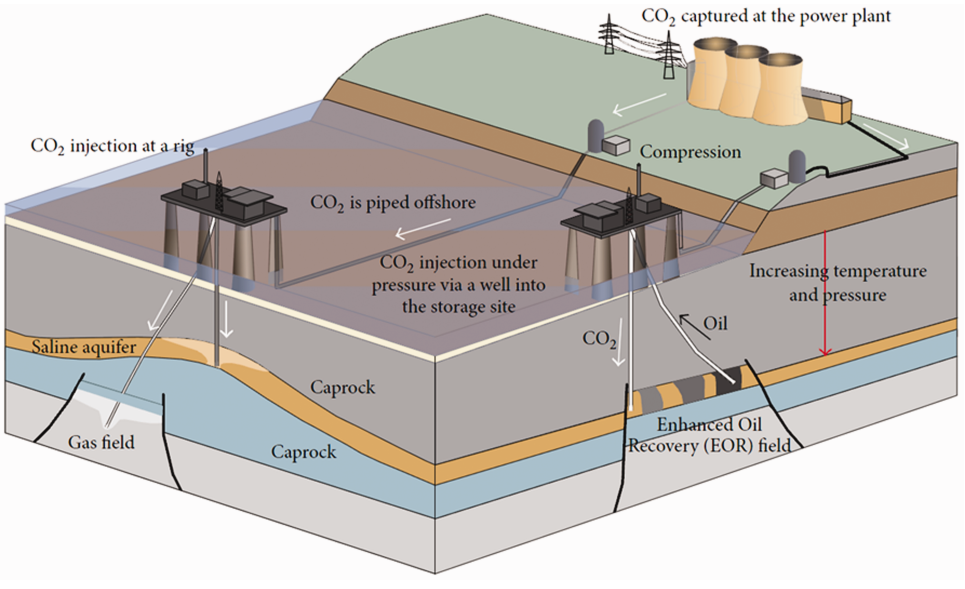


Figure 1. Schematic of CCS–EOR infrastructures (Sheng et al., 2015).

The equipment lease fee and other costs, which are dependent on reservoir site, were adopted from the work of Ettehadtavakkol et al. (2014).

Compressor and pump. The compression procedure is significant for transporting CO_2 from the capture site to the oil field. The compressor and pump are two main facilities that boost CO_2 pressure. The compressor is initially used to boost CO_2 pressure to its supercritical pressure for transport. Then, CO_2 can be delivered through the pipeline as a supercritical dense fluid. The pump is used to further increase the CO_2 pressure to injection pressure.

To adopt the compression procedure, equations (12) to (17) are referred from Mohitpour et al. (2000) and McCollum and Ogden (2006). They proposed the compression ratio (CR) as follows

$$CR = \left(\frac{p_{\text{discharge}}}{p_{\text{inlet}}}\right)^{\frac{1}{N}}, \quad CR \leq 6 \tag{12}$$

where

N = number of compression stages;
$p_{\text{discharge}}$ = discharge pressure (MPa); and
p_{inlet} = inlet pressure (MPa).

CAPEX and OPEX concepts were considered in this study. CAPEX for the compressor is calculated through the following equation

$$C_{\text{comp.}} = m_{\text{train}} N_{\text{train}} \left[\begin{array}{l} (0.13 \times 10^6)(m_{\text{train}})^{-0.71} + \\ (1.40 \times 10^6)(m_{\text{train}})^{-0.60} \ln\left(\frac{p_{\text{cut-off}}}{p_{\text{initial}}}\right) \end{array} \right] \tag{13}$$

where

$C_{\text{comp.}}$ = CAPEX of compressor ($);
m_{train} = CO_2 mass flow rate through each compressor train (kg/s);
N_{train} = number of parallel compressor trains;
$p_{\text{cut-off}}$ = pressure at which compression switches to pumping (MPa); and
p_{initial} = initial pressure of CO_2 directly from the capture system (MPa).

Like the compressor, CAPEX of the pump is calculated as

$$C_{\text{pump}} = 1.11 \times 10^6 \left(\frac{w_{\text{pump}}}{1000}\right) + 0.07 \times 10^6 \tag{14}$$

where

C_{pump} = CAPEX of pump ($) and
w_{pump} = pumping power requirement (kW).

Annual OPEX for the compressor and pump, $O_{\text{comp. and pump}}$, consists of annual operating and maintenance costs, $O\&M_{\text{annual}}$; and electric power costs, HP and w_{pump}. $O\&M_{\text{annual}}$ is calculated as follows

$$O\&M_{\text{annual}} = O\&M_{\text{factor}}(C_{\text{comp.}} + C_{\text{pump}}) \tag{15}$$

where

$$O\&M_{\text{factor}} = 0.04$$

Electric power costs for the compressor and pump are also considered. Electricity power cost is calculated as the product of power use and electricity cost. Compressor power use, HP, can be obtained from the following equation

$$HP = 0.0857\frac{K}{K-1}T_1\left[\left(\frac{p_2}{p_1}\right)^{\frac{K-1}{K}} - 1\right] \tag{16}$$

where
HP = adiabatic power requirement (HP/MMSCFD);
K = adiabatic gas exponent;
T_1 = suction temperature (R);
p_1 = suction pressure (psia);
p_2 = discharge pressure (psia); and
$\frac{p_2}{p_1}$ = compression ratio.

Pump power use can be expressed as follows

$$w_{\text{pump}} = \frac{(1000)(10)}{(24)(36)}\left[\frac{m(p_{\text{final}} - p_{\text{cut-off}})}{\rho\eta_{\text{pump}}}\right] \tag{17}$$

where
m = CO_2 mass flow rate (tons/day);
ρ = gas density (kg/m^3); and
η_{pump} = compressor efficiency.

Transportation. In CO_2 flooding, CO_2 flows through a pipeline. In this study, it was assumed that only OPEX for the pipeline was the operator's responsibility, as was true in a previous study (Ettehadtavakkol et al., 2014). McCollum and Ogden (2006) suggested equations for estimating onshore pipeline annual OPEX, O_{pipeline}, as follows

$$C_{\text{pipeline}} = 9970F_LF_Tm^{0.35}L^{1.13} \quad \text{and} \tag{18}$$

$$O_{\text{pipeline}} = O\&M_{\text{factor}}C_{\text{pipeline}} \tag{19}$$

where
F_L = location factor, UK = 1.2, USA/Canada/Europe/Japan/Australia = 1.0;
F_T = terrain factor, cultivated land = 1.1, grassland = 1.0, wooded = 1.05;
C_{pipeline} = pipeline CAPEX ($);

$$O\&M_{\text{factor}} = 0.025$$

m = mass flow rate (kg/s); and
L = pipeline length (km).

For ease of calculation, F_L, F_T, and L were assumed to be 1.0, 1.0, and 100 km, respectively.

NPV calculation. Equations (20) to (22) show the calculation of CAPEX and OPEX of overall economical consideration

$$\mathrm{CAPEX}_{\mathrm{total}} = \begin{pmatrix} C_{\mathrm{comp.}} + C_{\mathrm{pump}} + C_{\mathrm{minor\,cost}} \\ +C_{\mathrm{surface\,equipment}} + C_{\mathrm{CO_2}} + C_{\mathrm{LPG}} \end{pmatrix} \tag{20}$$

$$\mathrm{OPEX}_{\mathrm{annual}} = \begin{pmatrix} O_{\mathrm{comp.\,and\,pump}} + O_{\mathrm{minor\,cost}} \\ +O_{\mathrm{surface\,equipment}} + O_{\mathrm{pipeline}} \end{pmatrix}, \text{and} \tag{21}$$

$$\mathrm{OPEX}_{\mathrm{total}} = \sum_i \frac{\mathrm{OPEX}_{\mathrm{annual}}}{(1+r)^i} \tag{22}$$

where
$\mathrm{CAPEX}_{\mathrm{total}}$ = total CAPEX ($);
$C_{\mathrm{comp.}}$ = compressor CAPEX ($);
C_{pump} = pump CAPEX ($);
$C_{\mathrm{minor\,cost}}$ = minor cost CAPEX ($);
$C_{\mathrm{surface\,equipment}}$ = surface facility CAPEX ($);
$C_{\mathrm{CO_2}}$ = CO_2 purchase charge ($);
C_{LPG} = LPG purchase charge ($);
$\mathrm{OPEX}_{\mathrm{annual}}$ = annual OPEX ($);
$\mathrm{OPEX}_{\mathrm{total}}$ = total OPEX ($);
$O_{\mathrm{comp.\,and\,pump}}$ = compressor and pump annual OPEX ($);
$O_{\mathrm{minor\,cost}}$ = minor annual OPEX cost ($);
$O_{\mathrm{surface\,facility}}$ = surface facility annual OPEX ($); and
O_{pipeline} = pipeline annual OPEX ($).

Revenue in this study was obtained from two major sources: oil recovery and CO_2 geological storage carbon tax credit. Discounted revenue from oil recovery is calculated as follows

$$\text{Discounted revenue}_{\text{oil recovery}} = \sum_i \frac{q_{\text{oil, month}}}{(1+r)^i} \tag{23}$$

where
i = monthly period (month);
r = monthly discount rate; and
$q_{\text{oil, month}}$ = monthly oil production (bbl/month).
Discounted revenue from CCS carbon credit is expressed as follows

$$\text{Discounted revenue}_{\text{CCS}} = \frac{S_{\mathrm{CO_2}}(\text{tax credit})}{(1+r)^{(\text{month})(\text{year})}} \tag{24}$$

where

S_{CO_2} = stored CO_2 at the end of the project (ton).

NPV is calculated by comparing revenue and cost and is briefly expressed as follows

$$\mathrm{NPV} = \begin{bmatrix} (\text{Discounted revenue}_{\mathrm{CCS}} + \text{Discounted revenue}_{\mathrm{oil}}) \\ -(\mathrm{CAPEX}_{\mathrm{total}} + \mathrm{OPEX}_{\mathrm{total}}) \end{bmatrix} \tag{25}$$

Results

Fluid modeling

Fluid properties and relative permeability curves were adopted from the work of Ghomian (2008). EOS parameters for pseudo-components are listed in Table 1, and relative permeability curves are presented in Figures 1 and 2. Once the fluid model was developed and MMP was estimated by slim-tube simulation, the results were matched with given MMP data of 1500 psia at a given temperature. Results and interpretation of the slim-tube simulation are shown in Figure 3, with a slope change around 1500 psia and exact MMP was of 1478 psia. These results are acceptable in comparison to the given MMP data of 1500 psia.

Model description

CCS–EOR was applied to a single-layer, two-dimensional reservoir model. A five-spot model was chosen with a 720 ft × 720 ft × 100 ft size of one quarter and reservoir properties as shown in Table 2. Since the reservoir was deeper than 1800 ft, it was applicable to CCS–EOR (Klins, 1984; Kovscek, 2002; Shaw and Bachu, 2002; Taber et al., 1997). The injection scenario was planned to combine five years of pre-water flooding and 20 years of WAG injection with a cycle of six months. For pre-water injection, water was injected at a rate of 300 bbl/day; for the WAG process, water and gas were injected at a rate of 300 bbl/day and 35,760 ft^3/day of CO_2, respectively, with 0–0.15 mol fraction of additional LPG in each case. One ˆPV of water was injected for 10 years during pre-water injection. Since CO_2 is a highly compressible fluid, an injection rate of 1 PV for 10 years under near-miscible conditions was chosen. The injector and producer were located at the corners of the model, which were diagonally positioned.

Table 1. EOS parameters for pseudo-components (Ghomian, 2008).

Properties \ Component	CO_2	C_1	C_{2-3}	C_{4-6}	C_{7-16}	C_{17-29}	C_{30+}
Initial composition	0.0192	0.0693	0.1742	0.1944	0.3138	0.1549	0.0742
p_c (atm)	72.799	45.4	44.932	33.238	20.676	15.675	15.636
T_c (K)	303.89	166.67	338.34	466.12	611.12	777.78	972.23
Acentric factor	0.225	0.008	0.126	0.244	0.639	1.000	1.281
M_w (g/gmol)	44.010	16.043	36.013	70.520	147.18	301.48	562.81
Volume shift	0.14	–0.15	–0.01	–0.04	0.06	0.18	0.30
Parachor	49.00	71.000	135.00	231.62	439.15	788.22	1,112.5

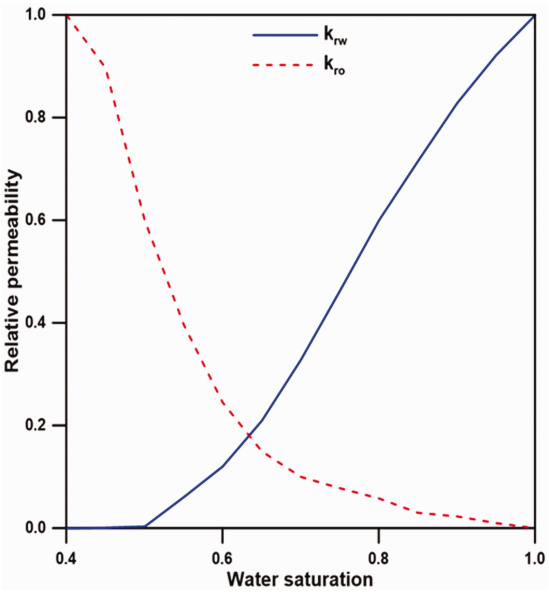


Figure 2. Water-oil relative permeability curves (Ghomian, 2008).

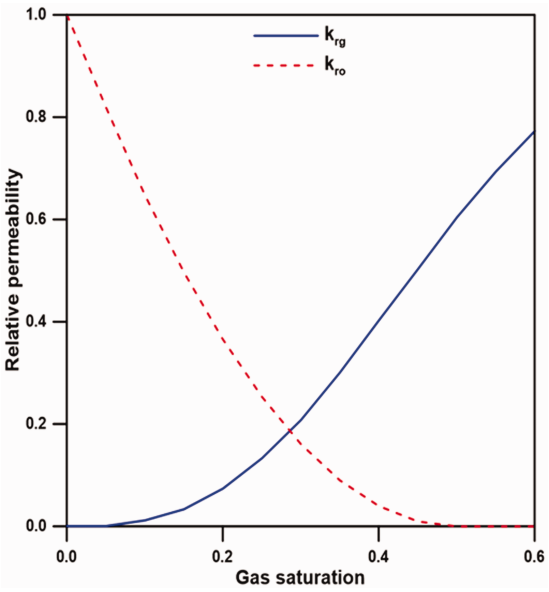


Figure 3. Gas-liquid relative permeability curves (Ghomian, 2008).

Miscibility adjustment through LPG addition

The miscibility condition was also adjusted through the addition of LPG, which was composed of half propane and half butane. Propane and butane prices were introduced from the

Table 2. Reservoir model properties.

Properties	*Values*
Reservoir size (ft^3)	51,840,000
Porosity	0.3
Horizontal permeability (md)	70
Initial pressure (psia)	1500
Depth to reservoir top (ft)	3000

Table 3. MMPs derived from slim-tube simulations depending on amount of LPG added (psia).

LPG addition (%)	*MMP*
0	1478
1	1429
2	1427
3	1420
4	1412
5	1402
6	1388
7	1373
8	1359
9	1347
10	1339
11	1330
12	1319
13	1307
14	1292
15	1283

OPIS North America LPG Report (OPIS, 2017). Based on the pressure-controlled immiscible CCS–EOR model, LPG was injected at different mole fractions from 0 to 15% with CO_2 as a solvent. The amount of injected CO_2 remained constant, while additional LPG produced a larger slug for a higher LPG mole percent. Economic evaluation was then carried out for the models with different LPG mole fractions in injection gas.

Since LPG acts as an intermediate component in the CO_2-oil phase diagram, adding LPG into the CO_2 stream resulted in a lower MMP between oil and CO_2-LPG gas than that of oil and CO_2 only. MMP data obtained by slim-tube simulations between oil and CO_2-LPG gas are listed in Table 3 with respective mole fraction of LPG. As more LPG is added into CO_2 stream, the MMP becomes low. For LPG-CO_2 injection, it was easier to achieve miscible conditions at the same pressure and temperature conditions as for CO_2 injection. The case of 15% LPG in injection gas had an MMP of 1283 psia, which was 195 psia lower than that of the 0% LPG injection case. The MMP change must be considered since it affects not only oil recovery and CO_2 sequestration but also NPV.

Enhanced oil recovery. Once CO_2 was injected into the reservoir, it started to interact with oil. Mixing with CO_2 resulted in lighter, easier flowing, and swelled oil. With greater miscibility

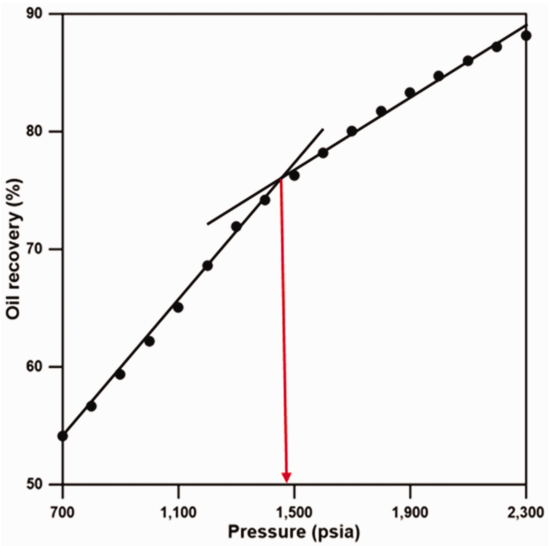


Figure 4. Results of MMP measurements using a slim-tube simulation.

between oil and injected gas, the IFT decreased. Increased reservoir pressure as well as decreased MMP by LPG injection produced miscible conditions. Figure 4 shows IFT change of cases with LPG fractions of 0, 5, 10, and 15% at the CO_2 swept zone. First, IFT remained zero since injected gas had not yet arrived and only oil existed at this location. Once CO_2 affected the oil at this location, the IFT started to increase. The IFT between oil and gas was lower in miscibility at earlier stages but higher at later stages due to influx of heavy fractions left behind when the gas removed intermediate fractions of oil through vaporization. The IFT change affected the shape of the relative permeability curves, as presented in Figure 5. Modification of the liquid–gas relative permeability curve due to the decreased IFT between oil and gas allowed easier flow.

Viscosity reduction is one of the major mechanisms of CO_2-EOR. With increasing addition of LPG to injection gas, oil viscosity decreased. Figure 6 shows viscosity changes for cases with LPG fractions of 0, 5, 10, and 15% at the CO_2 swept zone. Oil viscosity remained constant at the earlier stage since no gas flow had arrived. Once the gas reached this point, oil viscosity decreased to the minimum. The case of 15% LPG had the lowest oil viscosity of 0.08 cp, while the case of 0% LPG mole faction had a value of 0.14 cp. After this reduction, oil viscosity started to increase due to influx of heavy fractions. The lowest IFT and viscosity values at this location are listed in Table 4.

Figure 7 shows the oil recovery factor of every case. Increased addition of LPG injection led to higher miscibility and lower viscosity and IFT, which resulted in higher oil recovery. Since producer BHPs were fixed for every case, oil recovery factor curves showed an increasing tendency with the addition of LPG. The case of 14% LPG injection produced 15% more oil than the 0% LPG injection case.

CO_2 sequestration. Figure 8 shows the amount of sequestrated CO_2 at the last moment as a function of LPG mole fraction, showing a different tendency than the pressure-controlled CCS–EOR cases. Since the producer bottom hole pressure was fixed, earlier breakthrough,

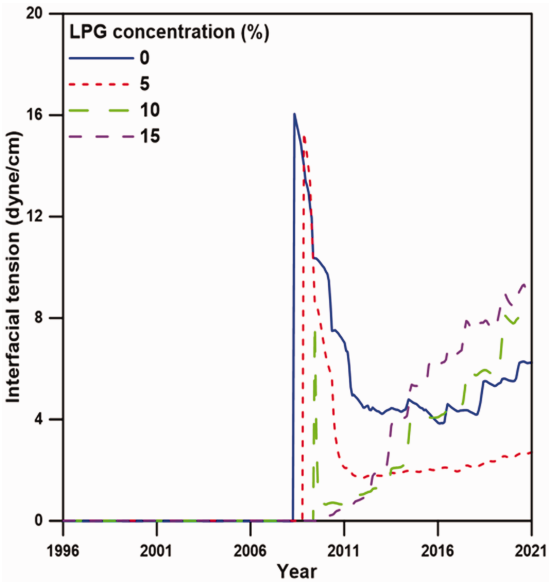


Figure 5. IFT changes at the CO_2-swept zone with LPG addition into the injection gas.

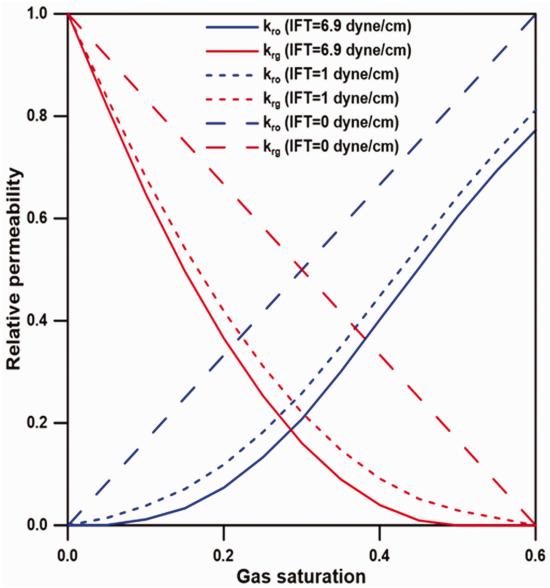


Figure 6. Gradual transition of relative permeability curves due to decreased IFT.

which caused major differences in sequestered CO_2 in pressure-controlled miscibility adjustment cases, had minor effects on these cases. However, the greater was the miscibility, the greater was the mixing of gaseous CO_2, which had the potential to be trapped by trapping mechanisms, with oil.

Table 4. Lowest IFT and oil viscosity values at the CO_2 swept zone depending on LPG addition.

LPG addition (%)	*IFT (dyne/cm)*	*Viscosity (cp)*
0	3.85	0.14
1	3.20	0.13
2	2.89	0.13
3	2.38	0.12
4	2.01	0.12
5	1.69	0.11
6	1.45	0.11
7	1.18	0.11
8	0.93	0.10
9	0.71	0.09
10	0.65	0.09
11	0.56	0.09
12	0.36	0.09
13	0.21	0.08
14	0.14	0.08
15	0.08	0.08

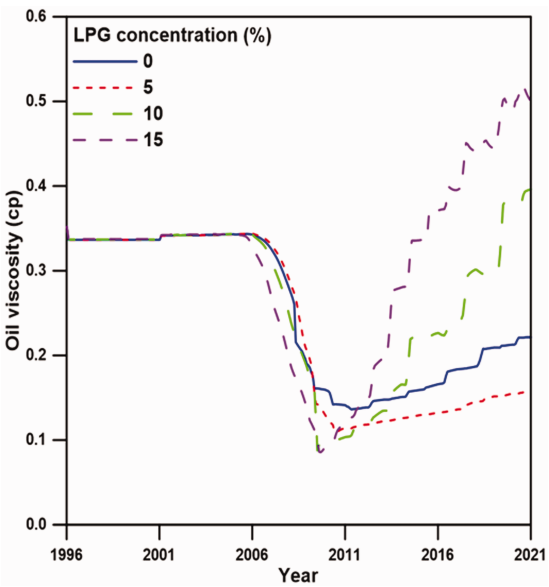


Figure 7. Oil viscosity changes at the CO_2-swept zone with LPG concentration in the injection gas.

Amount of dissolved CO_2 into water had a decreasing tendency as miscibility increased since the fugacity of gaseous CO_2, which acts as a major parameter in Henry's law, decreased. Residually trapped CO_2 was primarily dependent on saturation of gaseous CO_2. However, the amount of gaseous CO_2 was reduced, resulting in reduction of residually trapped CO_2.

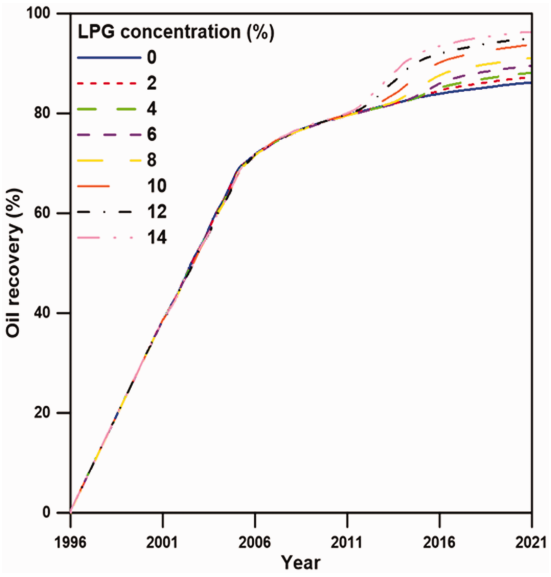


Figure 8. Oil recovery with LPG concentration in the injection gas.

Table 5. Cost of infrastructure in cases with increasing LPG addition into the injection gas ($).

	Compressor		*Pipeline*	
LPG addition (%)	*CAPEX*	*OPEX*	*CAPEX*	*OPEX*
0	4,340,817	264,714	6,230,677	155,767
1	4,358,190	265,410	7,625,368	190,634
2	4,375,809	266,114	8,018,026	200,451
3	4,393,682	266,829	8,304,671	207,616
4	4,411,814	267,555	8,541,264	213,532
5	4,430,213	268,290	8,747,724	218,693
6	4,448,884	269,037	8,934,100	223,353
7	4,467,834	269,795	9,105,440	227,636
8	4,487,072	270,565	9,265,237	231,631
9	4,506,605	271,346	9,379,256	234,482
10	4,526,439	272,140	9,499,693	237,492
11	4,546,585	272,945	9,619,392	240,485
12	4,567,049	273,764	9,725,242	243,131
13	4,587,841	274,596	9,822,970	245,574
14	4,608,970	275,441	9,892,626	247,316
15	4,630,446	276,300	9,964,710	249,117

NPV calculation. Propane and butane prices were assumed to be $507.324 and $462.05/ton, respectively (OPIS, 2017). Since LPG was very expensive compared to CO_2, produced LPG was recycled by separation in a separator, transportation to a compression site, transportation back to a reservoir, and re-injection. Pipeline to transport LPG from reservoir to

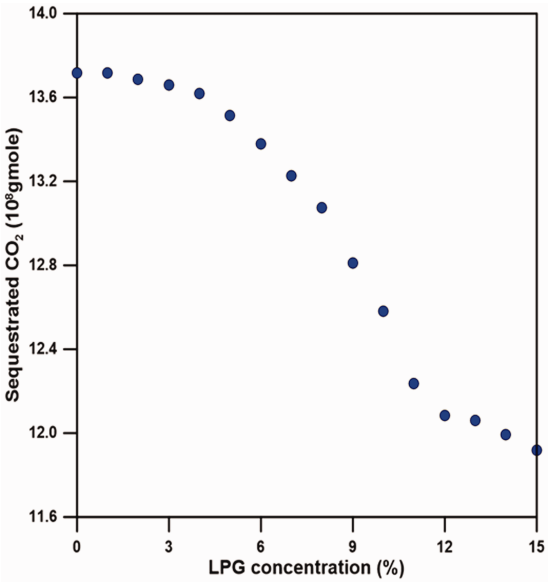


Figure 9. Amount of sequestrated CO_2 as a function of LPG concentration.

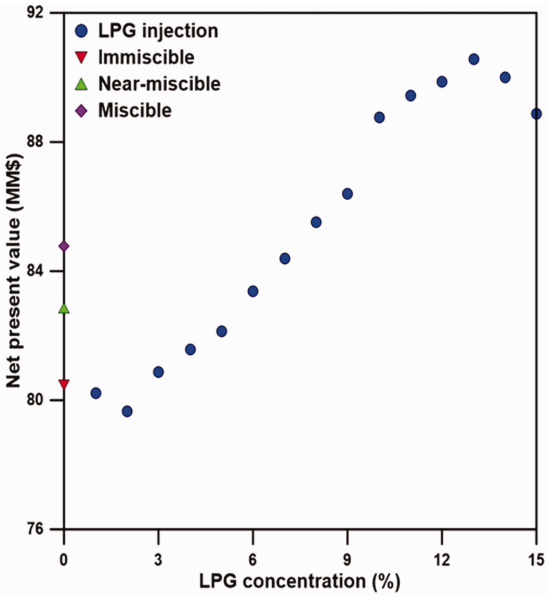


Figure 10. NPV as a function of LPG concentration.

compression site was constructed and considered in NPV calculation as CAPEX and OPEX. In compression, the adiabatic gas exponent of LPG was determined to be 1.28, which was the same as that of CO_2. Also, the discount rate is 2.3% (Advanced Resources International, 2006). Table 5 shows the CAPEX and OPEX of every case. Since WHPs of gas injectors in

every case were around 1100 psia, a pump was not installed. As mole fraction of LPG increased, injection mass rate increased, which led to increase in CAPEX and OPEX.

Purchase of additional butane was not needed until 7% LPG mole fraction. Cases with LPG composition of 8% or more needed additional butane since the amount of injected butane exceeded the produced butane. Likewise, additional propane was needed in cases with LPG composition of 13% or more.

Figure 9 shows NPV as a function of mole fraction and of immiscible, near miscible, and miscible cases. Oil recovery increased and NPV decreased from LPG mole fractions of 0–2% since compression cost increased due to the higher mass flow rate and addition of a pipeline. From LPG mole fractions of 2–13%, NPV increased considerably due to the miscibility effect. NPV started to decrease from 13 to 15% since the purchasing and injecting prices of required LPG exceeded the price of oil produced. As a result, the highest NPV had the value of \$90,572,302 when 13% of LPG is added.

Conclusions

Comprehensive CCS–EOR models were developed and analyzed to evaluate economic feasibility. Additional oil was produced by IFT, viscosity reduction, and relative permeability change, while CO_2 was sequestrated through solubility trapping, residual trapping, and free CO_2. Economic evaluations were performed considering revenues and costs.

Immiscible, near miscible, and miscible cases were characterized through the addition of LPG. Further reduction of IFT and oil viscosity resulted in higher oil recovery with LPG. Since a larger amount of CO_2 was mixed with oil by LPG addition, eventually producing a mixture with oil, a smaller amount of CO_2 was sequestrated. Cases of 1–2% LPG addition had a lower NPV than 0% (immiscible case), since costs from the additional infrastructure for LPG injection exceeded additional revenue. However, LPG addition of 3–13% showed gradually increased NPV, with a maximum of 91 MM\$. Finally, NPVs from LPG addition of 14–15% decreased due to costs exceeding revenues.

In this study, integrated CCS–EOR models based on economic analysis have been developed and applied for various operating conditions. It overcomes the limitations of previous studies that have not considered the effect of miscibility on economic feasibility of CCS–EOR. The developed model can be extended for the optimum field application with the optimization of various operating factors such as WAG ratio, injection scheme, and LPG composition.

Declaration of conflicting interests

The author(s) declared no potential conflicts of interest with respect to the research, authorship, and/or publication of this article.

Funding

The author(s) disclosed receipt of the following financial support for the research, authorship, and/or publication of this article: Dr Jinhyung Cho was partially supported by the National Research Foundation of Korea (NRF) (Grant No. 2019R1C1C1002574) and Korea Gas Corporation (KOGAS).

ORCID iD

Kun S Lee https://orcid.org/0000-0003-4735-1660

References

Advanced Resources International (2006) Basin Oriented Strategies for CO_2 Enhanced Oil Recovery: East & Central Texas. Report, US Department of Energy, USA, February.

Abdel-Aal HK and Alsahlawi MA (2013) *Petroleum Economics and Engineering*. Boca Raton: CRC Press.

Alvarado V and Manrique E (2010) Enhanced oil recovery: An updated review. *Energies* 3: 1529.

Appiah MO (2018) Investigating the multivariate granger causality between energy consumption, economic growth and CO_2 emissions in Ghana. *Energy Policy* 112: 198–208.

Araujo YC, Araujo M, Guzman H, et al. (2001) Effect of the spreading coefficient on two-phase relative permeability. In: SPE international symposium on oilfield chemistry, Houston, TX, USA, 13–16 February 2001.

Bardon C and Longeron DG (1980) Influence of very low interfacial tensions on relative permeability. *Society of Petroleum Engineers Journal* 20(5): 391–401.

Bastianin A, Galeotti M and Manera M (2017) Oil supply shocks and economic growth in the Mediterranean. *Energy Policy* 110: 167–175.

Blunt MJ (2000) An empirical model for three-phase relative permeability. In: SPE annual technical conference and exhibition, Houston, TX, USA, 3–6 October 1999.

BP (2018) BP energy outlook: 2018 edition. Report, BP, UK, February.

Dong M, Huang S and Srivastava R (2000) Effect of solution gas in oil on CO_2 minimum miscibility pressure. *Journal of Canadian Petroleum Technology* 39(11): 61.

Ettehadtavakkol A, Lake LW and Bryant SL (2014) CO_2 EOR and storage design optimization. *International Journal of Greenhouse Gas Control* 25: 79–92.

Exxonmobil (2018) Outlook for energy: A view to 2040. Report, Exxonmobil, USA, February.

Ghomian Y (2008) *Reservoir simulation studies for coupled CO_2 sequestration and enhanced oil recovery*. PhD Thesis, University of Texas at Austin, TX, USA.

Harvey AH (1996) Semiempirical correlation for Henry's constants over large temperature ranges. *AIChE J* 42(5): 1491–1494.

Hasan MMF, First EL, Boukouvala F, et al. (2015) A multi-scale framework for CO_2 capture, utilization, and sequestration: CCUS and CCU. *Computers & Chemical Engineering* 81: 2–21.

Holtz MH (2002) Residual gas saturation to aquifer influx: A calculation method for 3-D computer reservoir model construction. In: *SPE gas technology symposium*, Calgary, Alberta, Canada, 30 April–2 May 2002.

IEA (2019) Transforming Industry through CCUS. Report, IEA, France, May.

Jamaloei BY (2015) The effect of interfacial tension on two-phase relative permeability: A *review*. *Energy Sources, Part A: Recovery, Utilization, and Environmental Effects* 37(3): 245–253.

Jerauld GR (1997) General three-phase relative permeability model for Prudhoe Bay. *SPE Reservoir Engineering* 12(4): 255–263.

Killough JE (1976) Reservoir simulation with history-dependent saturation functions. *Society of Petroleum Engineers Journal* 16(1): 37–48.

Klins MA (1984) *Carbon Dioxide Flooding: Basic Mechanisms and Project Design*. Boston: International Human Resources Development Corporation.

Kovscek AR (2002) Screening criteria for CO_2 storage in oil reservoirs. *Petroleum Science and Technology* 20(7–8): 841–866.

Land CS (1968) Calculation of imbibition relative permeability for two- and three-phase flow from rock properties. *Society of Petroleum Engineers Journal* 8(2): 149–156.

Larsen JA and Skauge A (1998) Methodology for numerical simulation with cycle-dependent relative permeabilities. *SPE J* 3(2): 163–173.

Lenhard RJ and Oostrom M (1998) A parametric model for predicting relative permeability-saturation-capillary pressure relationships of oil-water systems in porous media with mixed wettability. *Transport in Porous Media* 31: 109–131.

Lenhard RJ and Parker JC (1987) A model for hysteretic constitutive relations governing multiphase flow: 2. Permeability-saturation relations. *Water Resources Research* 23(12): 2197–2206.

Leung DYC, Caramanna G and Maroto-Valer MM (2014) An overview of current status of carbon dioxide capture and storage technologies. *Renewable and Sustainable Energy Reviews* 39: 426–443.

Li YK and Nghiem LX (1986) Phase equilibria of oil, gas and water/brine mixtures from a cubic equation of state and Henry's law. *The Canadian Journal of Chemical Engineering* 64(3): 486–496.

McCollum DL and Ogden JM (2006) Techno-economic models for carbon dioxide compression, transport, and storage & correlations for estimating carbon dioxide density and viscosity. Report, University of California, USA, October.

McDougall SR, Salino PA and Sorbie KS (1997) The effect of interfacial tension upon gas-oil relative permeability measurements: Interpretation using pore-scale models. In: *SPE annual technical conference and exhibition*, San Antonio, Texas, USA, 5–8 October 1997, pp.791–803.

Mohitpour M, Golshan H and Murray A (2000) *Pipeline Design & Construction: A Practical Approach*. New York: ASME Press.

Nunez-Lopez V, Gil-Egui R and Hosseini SA (2019) Environmental and operational performance of CO_2-EOR as a CCUS technology: A Cranfield example with dynamic LCA. *Energies* 12(3): 448.

OPIS (2017) OPIS North America LPG report. Report, OPIS, USA, December.

Peng DY and Robinson DB (1976) A new two-constant equation of state. *Industrial & Engineering Chemistry Fundamentals* 15(1): 59–64.

Reid RC, Prautsnitz JM and Sherwood TK (1977) *The Properties of Gases and Liquids*. New York: McGraw-Hill.

Rognmo AU, Fredriksen SB, Alcorn ZP, et al. (2019) Pore to core EOR upscaling for CO_2 foam for CCUS. *Society of Petroleum Engineers Journal* 24(6): 1–11.

Shaw JC and Bachu S (2002) Screening, evaluation and ranking of oil reserves suitable for CO_2 flood EOR and carbon dioxide sequestration. *Journal of Canadian Petroleum Technology* 41(9): 61. 51.

Sheng Y, Sousani M, Ingham D, et al. (2015) Recent developments in multiscale and multiphase modelling of the hydraulic fracturing process. *Mathematical Problems in Engineering* 2015: 1–15.

Taber JJ, Martin FD and Seright RS (1997) EOR screening criteria revisited part 1: Introduction to screening criteria and enhanced recovery field projects. *SPE Reservoir Engineering* 12(3): 189–198.

Tiba S and Omri A (2017) Literature survey on the relationships between energy, environment and economic growth. *Renewable and Sustainable Energy Reviews* 69: 1129–1146.

Walheer B (2018) Labour productivity growth and energy in Europe: A production-frontier approach. *Energy* 152: 129–143.

Yongmao H, Zenggui W, Binshan J, et al. (2004) Laboratory investigation of CO2 flooding. In: Annual SPE international technical conference and exhibition, Abuja, Nigeria, 2–4 August 2004.